

The influence of residual stresses implicated via cure volume shrinkage on CF/VEUH—composites

PATRICK ROSSO*

*Institut für Verbundwerkstoffe GmbH, Technical University Kaiserslautern,
Erwin Schrödinger Str. 58, 67663 Kaiserslautern, Germany*

BODO FIEDLER

*Polymer/Composite Section, Technical University Hamburg-Harburg, Nesspriel 5,
21129 Hamburg, Germany*

KLAUS FRIEDRICH

*Institut für Verbundwerkstoffe GmbH, Technical University Kaiserslautern,
Erwin Schrödinger Str. 58, 67663 Kaiserslautern, Germany*

KARL SCHULTE

*Polymer/Composite Section, Technical University Hamburg-Harburg, Nesspriel 5,
21129 Hamburg, Germany*

Published online: 12 January 2006

This paper presents a thermal finite element analysis (FEA) of a unidirectional carbon fibre reinforced vinylester urethane hybrid matrix system. The evolution of the thermal residual stresses due to the mismatch in the coefficient of thermal expansion (CTE) of the single components in the cooling phase have been investigated. Additionally, the cure volume shrinkage was implemented into the FE-model. The model allows the transition of the homogeneous unidirectional composite material properties on a microscopic spot, where the properties of the fibres and the matrix can be considered separately. It could be shown, that the cure volume shrinkage (CVS) has a dramatic effect on the fibre/matrix interface region due to radial compression stresses along the fibre. Further, this may lead to microcracking or fibre/matrix debonding before any kind of load is applied to the material.

© 2006 Springer Science + Business Media, Inc.

1. Introduction

It is well known, that carbon fibre reinforced vinylester composites possess lower mechanical properties than composite materials based on a typical epoxy matrix systems. One crucial factor for this phenomenon can be seen in the high residual stresses of these materials especially when high curing temperatures are demanded [1]. The majority of the residual stresses are generated during cooling down to room temperature due to the mismatch in the coefficient of thermal expansion (CTE) of the single components matrix and fibre. Nevertheless, a further deciding factor is often disregarded, namely the cure volume shrinkage of the matrix. Compared to epoxy systems, vinylesters usually exhibit higher cure volume shrinkage. As a result, residual stresses can be implicated [2–4]. It is the objective here, to study the effect of such stresses

by finite element analysis (FEA), using an existing and approved model [5, 6].

Since the curing of a thermoset material is always combined with a phase transition from liquid to solid, it is hard to tell when the evolution of residual stresses starts. In [7], it is shown how the stress free temperature can be calculated from a finite element-based process model, whereas in [8] the development of the polymer stiffness during a cure cycle was determined more or less in-situ. This field is, however, always combined with some uncertainties. Many publications exist on the influence of residual stresses on CF/Epoxy [9, 10] but the research work using vinylester (VE) as a matrix system for continuous fibre reinforced composites is rather limited. A numerical approximation of residual stresses associated with post-cure shrinkage in glass-fibre (GF) reinforced VE—tubes

* Author to whom all correspondence should be addressed.

showed, that the residual stresses tend to increase with increasing ratio of wall thickness to inner radius [11], which is a very valuable information to pipework designers in the industry. Furthermore, Andersson *et al.* [12] showed, that it seems likely, residual stresses causes irreversible matrix deformation and debonding in the curing phase of GF/VE. It was observed in [13], that CF/VE posses lower transverse tensile strength than GF/VE, which shows less intralaminar failures. This could be an indication, that the use of carbon fibres in VE has an even bigger impact on the formation of the residual stresses in the produced composite.

A vinylester-urethane hybrid resin system (VEUH) was used in order to combine a good corrosion and chemical resistance with a high thermal stability ($T_g \sim 240^\circ\text{C}$). Due to the dual crosslinking mechanism and a high network density, a loss in ductility has to be accepted. The system achieves a tensile fracture strain of only 2.5%. More details for this system are given in [14, 15]. In principal, the aim of this study is to show that the cure volume shrinkage can dramatically affect the interface properties due to radial compression stresses along the fibre.

2. Experimental

2.1. Materials and processing

As matrix material, a vinylester hybrid resin system from DSM-BASF Structural Resins (Zwolle, The Netherlands) was used. It consisted of the following parts: bisphenol-A based styrene-diluted VE of bismethacryloxy type (Daron XP 45-A-2, 100 parts) and novolac-based polymeric isocyanate (Daron XP 40-B-1, 38 parts). The hardener Lucidol CH 50 L (1.5 parts) was provided by AKZO-Nobel Chemicals GmbH (Düren, Germany). The resin was mixed at room temperature and afterwards cured in the following steps: 50°C for 15 min, 80°C for 15 min, 150°C for 30 min, and post-curing at 200°C for 60 min. The last post-cure step at 200°C is not considered in our FE-calculations since the resin is completely solid

at 150°C . The post-curing only benefits the mechanical properties of the VEUH at higher temperatures due to a higher crosslinking formed. The fibres used were PAN-based high tenacity carbon fibres, type Tenax HTA 5131 (standard oxidative treatment with epoxy sizing) from Tenax Fibers GmbH (Wuppertal, Germany).

The specimens used within this study were produced by filament wet-winding technique. The laminate consisting of 5 unidirectional plies was cured in an oven between two steel plates in a vacuum bag. The plates were cut off the plate after curing and the resulting winding-angle was about 1° at a thickness of ~ 2 mm. The resulting fibre volume fraction was measured to $52.3 \pm 5.1\%$ by ignition loss method.

2.2. Testing

Dynamic mechanical thermo analysis (DMTA) experiments were conducted on an Eplexor (Gabo Qualimeter). Viscoelastic material parameters such as mechanical loss factor and complex tensile Young's modulus ($\tan \delta$ and E^* , respectively) were determined in tensile loading parallel and transverse to the fibre direction over a broad temperature range (-100 to $+300^\circ\text{C}$) at a heating rate of $1^\circ\text{C}/\text{min}$ and a frequency of 10 Hz.

The coefficient of thermal expansion was measured by thermo mechanical analysis (TMA Mettler Toledo).

3. Finite element analysis

3.1. FE-model

To incorporate the dependence of the Young's modulus E on temperature into the FEA, the storage moduli from the DMTA were normalized to the room temperature values obtained by standard tensile tests, assuming that the influence of the temperature on both moduli is similar. In Fig. 1, the normalized moduli of the neat resin and composite, parallel and transverse to the fibre direction, are shown. With decreasing influence of

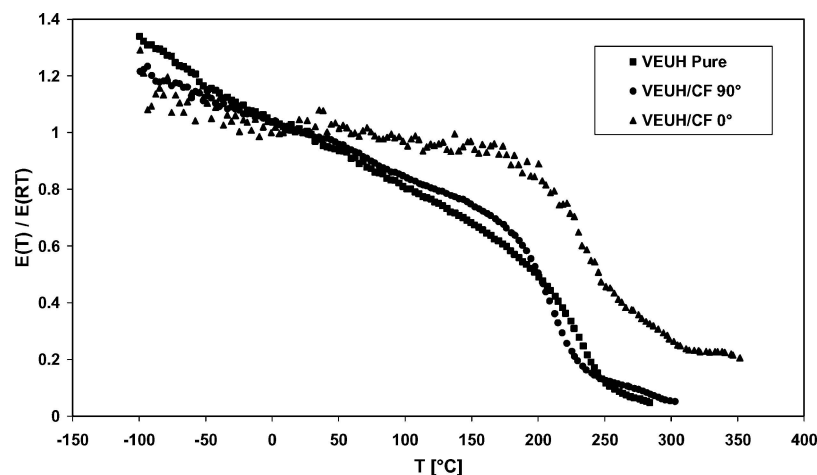


Figure 1 Normalized modulus of the neat VEHU resin and the unidirectional CF/VEUH composite in 0° - and 90° -direction obtained by DMTA at a frequency of 10 Hz in tensile mode.

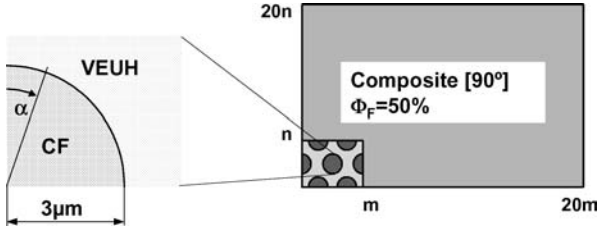


Figure 2 2-D plain strain FE Model (schematic).

the fibres (orientation), the loss in stiffness is affected more by the increasing temperature. The analyses of the thermal residual stresses were carried out using the commercial finite element code MARC/MentatTM. More assumptions are: (a) No creep is considered in the model. (b) Hexagonal fibre arrangement is assumed. (c) Perfect bonding between fibre and matrix. (d) The carbon fibres are orthotropic and behave linear elastic, whereas the matrix is isotropic, having a non-linear stress/strain behaviour with plastic deformation following the v. Mises criterion. The finite element model is shown schematically in Fig. 2. It consists of 2-dimensional plane strain elements. The microscopic area of fibre and matrix is surrounded by elements with homogenous properties of a unidirectional composite with transverse orientation (self consisted model). The volume fractions for both composite element areas were constant $V_f = 50\%$. The material properties used for the study are summarized in Table I. Most values were measured by the authors, however, missing values were taken directly from the suppliers data sheet or from literature. The elastic and thermal properties of the composite elements were calculated from the properties of fibre and matrix according to the rule of mixture [16].

3.2. Implementation of cure volume shrinkage

The cure volume shrinkage was determined to 5% by dilatometry [17]. Rheometric and conversion studies have been carried out [17] to clarify the reaction kinetics of

TABLE I Elastic and thermal properties of the HTA carbon fibre, the VEUH resin and the composite containing 50 vol% fibres

	Resin VEUH 20°C	HTA carbon fibre	Composite ($\Phi_F = 50\%$) 20°C
E_1 [GPa]	3000	235	119
E_2 [GPa]		15	6.9
E_3 [GPa]		15	6.9
G_{12} [GPa]		20	3.68
G_{23} [GPa]		5	3.53
G_{31} [GPa]		20	3.68
n_{12}	0.35	0.28	0.32
n_{23}		0.33	-0.02
n_{21}		0.02	0.02
α_1 [1/K]	55 E-6	-0.4 E-6	0.3
α_2 [1/K]		10 E-6	42 E-6
α_3 [1/K]		10 E-6	42 E-6

TABLE II Implementation of the CVS into the different FE-models

FE-model no.	Portion of total CVS (5%) in solid phase	α_m 150–100°C [1/K]	α_m 100–25°C [1/K]
1	0%	55×10^{-6}	55×10^{-6}
2	0.75%	105×10^{-6}	55×10^{-6}
3	1%	121.6×10^{-6}	55×10^{-6}
4	1.25%	138.3×10^{-6}	55×10^{-6}

the VEUH system. It was found, that the cure volume shrinkage occurs after the gel-point of the resin and thus after the phase transition from liquid to solid. However, it is a critical point to tell when the evolution of residual stresses starts. In our case, the stress free temperature was set to 150°C [1].

The proposed finite element model implements the cure volume shrinkage (CVS) of the matrix as a function of the coefficient of thermal expansion (CTE). The definition of the coefficients α and β at a constant pressure are for linear expansion:

$$\alpha = \frac{1}{l} \left(\frac{\delta l}{\delta T} \right)_P \quad (1)$$

and for volume expansion:

$$\beta = \frac{l}{V} \left(\frac{\delta V}{\delta T} \right)_P \quad (2)$$

where l means length, V means volume, P means pressure and T means temperature. Assuming the neat matrix to be an isotropic, homogeneous material, the volume expansion should follow $\beta = 3*\alpha$. This leads to:

$$\delta V = V_1*(3*\alpha)*\delta T, \quad (3)$$

V_1 = Volume before CVS

V_2 = Volume after CVS, $0.95*V_1$

As mentioned above, the CVS is 5% for the VEUH material. If V_2 is equal to $0.95*V_1$ and $\delta T = 50$ K, according to Equation 3, α can be calculated. Table II shows how the CTE is implemented in four different models assuming that the CVS appear in the solid phase between 150 and 100°C to an extent of 0.75, 1 and 1.25% shown in model 2, 3 and 4, respectively. For comparison the calculation without CVS was also done and is represented by model 1. Note, that 0.75, 1 and 1.25% only reflect a portion of the total CVS (5%) and these fractions were chosen randomly.

4. Results and discussion

Generally, the residual stresses here are build due to the mismatch in the CTE of the neat matrix and the carbon fibres. Fig. 3 illustrates the evaluation of the von Mises stresses in the matrix. Without CVS, model 1 shows a

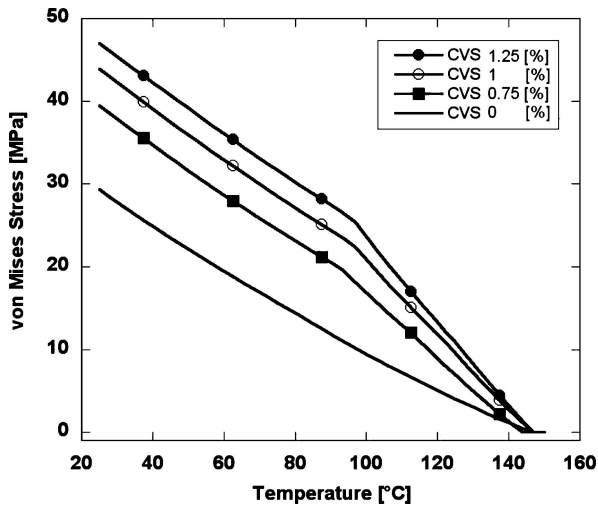


Figure 3 Evolution of von Mises Stresses during cooling from 150 to 25°C for the different FE-Models.

fairly linear increase up to 30 MPa, which is already very high considering the fact the tensile strength of the neat resin is only 70 MPa, and the transverse tensile strength of the composite is 25 MPa. The reason for this dramatic stress formation can be seen in the high thermal stability of this specific system, showing a high glass transition temperature of $T_g = 240^\circ\text{C}$. Therefore, the resulting Young's Modulus is relative high at the end of the curing and the entire cooling down process. That means the high stiffness at higher temperatures is predestined to induce high residual stresses. However, the v. Mises stress σ_{Mises} significantly increases when the CVS is additionally considered. Model 2, 3 and 4 deliver 38, 50 and 60% higher stresses, respectively. It is worth mentioning, that the assumption to implement the CVS in the solid phase to an extent of maximum 25% is rather conservative than overestimated.

The evolution of the equivalent plastic strain during cooling (Fig. 4) is similar to the stress development. In

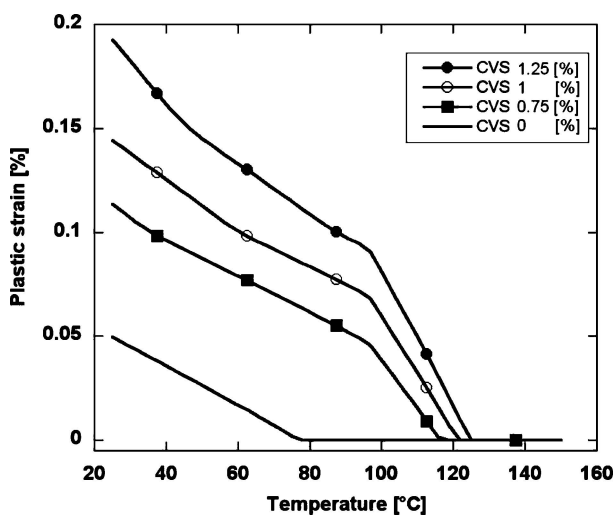


Figure 4 Formation of the equivalent plastic strain during cooling from 150 to 25°C for the different FE-Models.

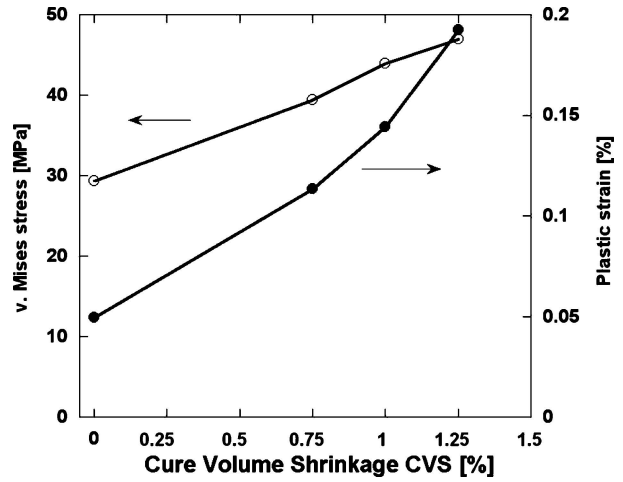


Figure 5 Dependency of the assumed amount of the total CVS in the solid phase on stress and strain.

all cases a plastic deformation start to form when the temperature dependent yield stress is reached. For the FE analysis, the yield stress of the matrix at room temperature was set to the resin strength. The yield stress decreases linear from $\sigma_y = 70$ to $\sigma_y = 18$ MPa at the stress free temperature of $T = 150^\circ\text{C}$. During the first step, when CVS is possible, the plastic deformation of the matrix starts below 130°C and increases linearly, at 100°C when the CVS is finished, the increase of plastic deformation is smaller with the cooling process. In case of no CVS the occurrence of plastic deformation is delayed and starts at about 80°C .

The influence of the cure volume shrinkage of the generation of stresses in the matrix with regard to its plasticity is summarized in Fig. 5. With increasing the CVS it can be seen that the resulting v. Mises stress increases linearly. The reason for this behaviour is that the plastic strain values are relatively small, and the effect on stress reduction is also small.

For no CVS and 1.25% CVS the radial- and hoop stress distribution at RT in the matrix of the discrete part of the FE-model is illustrated in Fig. 6. The distribution of the

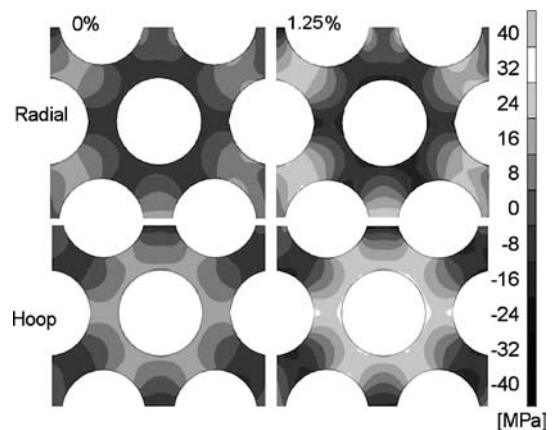


Figure 6 Distribution of the radial and hoop stress depending on the assumed amount of the total CVS in the solid phase.

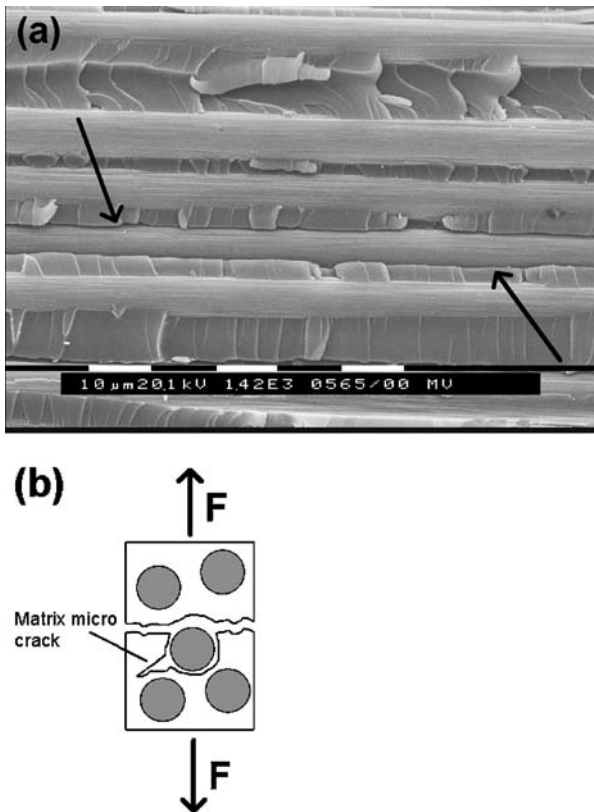


Figure 7 Debonded carbon fibre: scanning electron microscopy photograph (a) and schematic (b).

radial- and hoop stress refer to the centre of the median fibre, which is the origin of the cylindrical coordinate system. The fibres and the surrounding homogenized 90° composite are not shown. Locally, in the resin matrix tri-axial stresses are build up. During cooling in combination with the constraint of the neighbouring fibres, the matrix behaves as a stiffer elastic material than under uniaxial conditions (tensile test of dog bone specimens).

It can be concluded that at this regions microcracking occurs and may contribute to preliminary fibre/matrix debonding within the composite. Further, this debonded regions can help to decompose local stress concentrations. A scanning electron micrograph (SEM) from a dual cantilever beam specimen tested under mode-I loading is shown in Fig. 7a. Attention should be paid to the fibre indicated by the arrows and the fact, that the fibre is more or less lying in a matrix cave. The global failure mechanism as schematically shown in Fig. 7b is just partly responsible for this debonded region. As the strength of the fibre/matrix interface appears to be very low due to a poor fibre/matrix adhesion, matrix microcracks are able to deload the compression of the fibre when they growing to the interface.

A further example is shown in Fig. 8, which shows the fracture surface of a single embedded filament (CF) in a micro-tensile bar (as used for single fibre fragmentation). In this case, only a single fibre is considered, which is surrounded by a huge amount of bulk matrix. However,

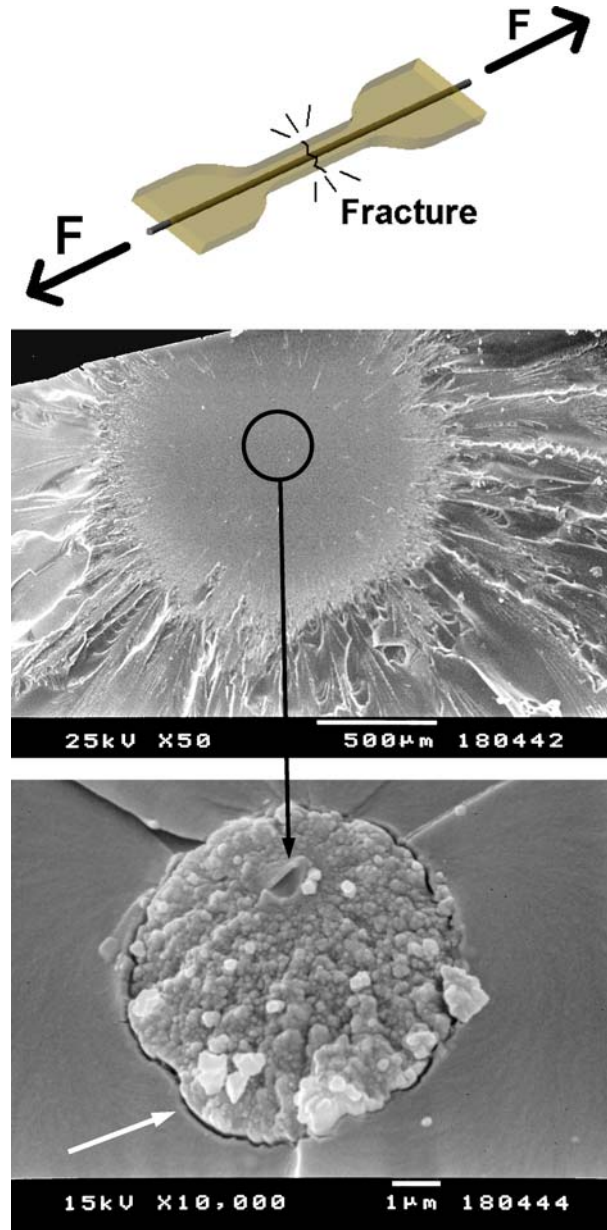


Figure 8 Fracture surface after tensile loading of a single embedded fibre (SEM).

the observed failure mechanism is supporting the FEM results. As it can be seen on a global view, the single fibre causes an enormous stress concentration, being responsible for the start of failure. After initiating, the matrix fails immediately in a brittle manner. Having a closer look on the fibre/matrix-interface region at higher magnifications demonstrates, that a fairly big “gap” was build around the fibre (white arrow). This can not only be ascribed to the fibre/matrix debonding during testing, but also due to some prior acting residual stresses.

5. Conclusion

In conclusion we showed by using an appropriate FE-model, that the implementation of 5% cure volume

shrinkage results in a dramatic increase of the residual stresses at the fibre/matrix interface region (up to 60%), when only 0.75–1.25% of the total CVS (5%) is assumed to occur in the solid phase. This could lead to microcracking preferably at the fibre/matrix interface region. It seems likely, that these high induced residual stresses do not allow as high transverse loading of the unidirectional laminate until the total failure occurs.

Acknowledgments

The authors gratefully acknowledge the support of the Deutsche Forschungsgemeinschaft (DFG FOR 360, Fr 675/32-3). Thanks are also addressed to DSM-BASF Structural Resins and Tenax Fibers GmbH, who kindly supplied the materials used in this study.

References

1. P. ROSSO and K. VARADI, "FE macro/micro analysis of thermal residual stresses and failure behaviour under transverse tensile load of VE/CF—Fibre bundle composites," *Composites Science and Technology*, accepted in January 2005.
2. L. XU, T. MASE and L. DRZAL, "Influence of cure volume shrinkage of the matrix resin on the adhesion between carbon fiber and vinyl ester resin," in Proceedings of 14th International Conference on Composite Materials ICCM-14 (San Diego, California, USA 2003) (on CD-ROM).
3. S. WIJSKAMP, R. AKKERMAN and E. A. D. LAMERS, "Residual stresses in non-symmetrical carbon/epoxy laminates," Proceedings of 14th International Conference on Composite Materials ICCM-14 (San Diego, California, USA 2003) (on CD-ROM).
4. C. LI, M. HOJJATI, A. JOHNSTON, K. C. COLE, D. DJOKIC and P. LEE-SULLIVAN, "Residual stress modelling in composite patch repairs employing a cure kinetics model with diffusion control," in Proceedings of 14th International Conference on Composite Materials ICCM-14 (San Diego, California, USA, 2003) (on CD-ROM).
5. B. FIEDLER, M. HOJO, S. OCHIAI, K. SCHULTE and M. OCHI, "Finite-element modeling of initial matrix failure in CFRP under static transverse tensile load," *Comp. Sci. Tech.* **61** (2001) 95.
6. B. FIEDLER, M. HOJO and S. OCHIAI, "The influence of thermal residual stresses on the transverse strength of CFRP using FEM," *Composites: Part A* **33** (2002) 1323.
7. K. M. NELSON, P. D. PUGLIANO and R. COURDJI, "Predicting residual stresses in composites," in Proceedings of 14th International Conference on Composite Materials ICCM-14 (San Diego, California, USA, 2003) (on CD-ROM).
8. M. S. MADHUKAR and B. FRANKS, "A new method to characterize stiffness in polymers," Proceedings of 14th International Conference on Composite Materials ICCM-14, (San Diego, California, USA, 2003) (on CD-ROM).
9. J. A. NAIRN, "Fracture mechanics of composites with residual thermal stresses," *J. Appl. Mech.* **64** (1997) 804.
10. K. JAYARAMAN and K. L. REIFSNIDER, "The interphase in unidirectional fiber-reinforced epoxies: effect on residual thermal stresses," *Comp. Sci. Tech.* **47** (1993) 119.
11. M. A. STONE, I. F. SCHWARTZ and H. D. CHANDLER, "Residual stresses associated with post-cure shrinkage in GRP tubes," *ibid.* **57** (1997) 47.
12. B. ANDERSSON, A. SJÖGREN and L. BERGLUND, "Micro- and meso-level residual stresses in glass-fiber/vinyl ester composites," *ibid.* **60** (2000) 2011.
13. C. WONDERLY, J. GRENESTEDT, G. FERNLUND and E. CEPUS, "Comparison of mechanical properties of glass fiber/vinyl ester and carbon fiber/vinyl ester composites," *Comp. Enging.: Part B* **36** (2005) 417.
14. P. ROSSO and K. FRIEDRICH, "Characterisation of different carbon fibre surface treatments and its effects on the interfacial failure behaviour of VEH-model composites," *Plastics, Rubber and Composites* **31** (2002) 134.
15. P. ROSSO, K. FRIEDRICH, C. LENZ and L. YE, "Effects of vinylester—Modification on the mechanical and interfacial properties of their carbon fibre reinforced—composites," *submitted to Composites Part A* in October 2004.
16. C. C. CHAMIS, "Simplified composite micromechanics equations for hygral, thermal and mechanical properties," *SAMPE Quarterly* (1984), 14.
17. N. JOST, *VERNETZUNG und Chemorheologie von Duromeren mit hybrider und interpenetrierender Struktur* (PhD-Thesis); edited by Prof. Dr.-Ing. Alois K. Schlarb, ISBN-3-934930-39-5, Kaiserslautern, 2004.

Received 13 February
and accepted 27 May 2005